

Review

Open Access



Making the most of computed tomography imaging in preoperative assessment and planning of abdomen-based flap breast reconstruction

Jisu Kim, Kyong-Je Woo[#] , Goo-Hyun Mun[#]

Department of Plastic Surgery, Samsung Medical Center, Sungkyunkwan University School of Medicine, Seoul 06351, South Korea.

[#]Authors contributed equally.

Correspondence to: Dr. Kyong-Je Woo, Dr. Goo-Hyun Mun, Department of Plastic Surgery, Samsung Medical Center, Sungkyunkwan University School of Medicine, 81 Irwon-ro, Gangnam-gu, Seoul 06351, South Korea. E-mail: economywoo@gmail.com; supramicro@gmail.com

How to cite this article: Kim J, Woo KJ, Mun GH. Making the most of computed tomography imaging in preoperative assessment and planning of abdomen-based flap breast reconstruction. *Plast Aesthet Res.* 2025;12:17. <https://dx.doi.org/10.20517/2347-9264.2024.157>

Received: 27 Nov 2024 **First Decision:** 15 Apr 2025 **Revised:** 12 May 2025 **Accepted:** 20 May 2025 **Published:** 28 May 2025

Academic Editor: Tine Engberg Damsgaard **Copy Editor:** Ting-Ting Hu **Production Editor:** Ting-Ting Hu

Abstract

Computed tomography angiography (CTA) offers substantial benefits for reconstructive surgeons in preoperative planning for abdomen-based flap procedures in breast reconstruction. The abdominal perforator-based autologous breast reconstruction has become the gold standard due to its superior cosmetic outcomes and high patient satisfaction. Meticulous preoperative planning is crucial for the success of deep inferior epigastric artery perforator (DIEP) flap breast reconstruction. In this context, CTA, recognized as the gold standard for perforator mapping, provides crucial insights into patient anatomy, optimizing flap design and elevation. This study aims to go beyond the role of CTA for perforator mapping and summarize the wealth of information that can be obtained from preoperative imaging tools for abdomen-based flaps in breast reconstruction. Such information not only aids in assessing the risk of postoperative complications but also supports the design of various flaps beyond DIEP. Furthermore, we will introduce the latest methods for utilizing this information to assist during preoperative planning and intraoperative decision making.

Keywords: Microsurgery, abdominal-based breast reconstruction, preoperative planning, computed tomography angiography



© The Author(s) 2025. **Open Access** This article is licensed under a Creative Commons Attribution 4.0 International License (<https://creativecommons.org/licenses/by/4.0/>), which permits unrestricted use, sharing, adaptation, distribution and reproduction in any medium or format, for any purpose, even commercially, as long as you give appropriate credit to the original author(s) and the source, provide a link to the Creative Commons license, and indicate if changes were made.



INTRODUCTION

In breast reconstruction, the autologous abdominal flap is considered the gold standard, with computed tomography angiography (CTA) primarily used for perforator mapping^[1]. This allows surgeons to identify deep inferior epigastric artery (DIEA) vascular anatomy, which expedites pedicle dissection and reduces operating time^[1,2]. However, the utility of CTA extends far beyond its traditional role in perforator mapping. By actively integrating this wealth of information into the preoperative planning process, surgeons can optimize flap design, better anticipate potential challenges, and reduce the likelihood of complications. This comprehensive approach underscores the evolving role of CTA as an indispensable tool for enhancing surgical outcomes in breast reconstruction.

Therefore, this paper aims to describe the range of data that CTA can provide when maximally utilized. While institutions may vary in the specific protocols and types of information they gather from CTA, we will share our routine approach to leveraging CTA data. Furthermore, this paper will outline the author's current intraoperative techniques for applying CTA insights and demonstrate how these findings can be translated into practical applications at each stage of the surgical process.

RISK ASSESSMENT

Sarcopenia assessment

The concept of sarcopenia was first introduced by Rosenberg in 1989 and has since gained recognition for its association with preoperative sarcopenia and postoperative morbidity^[3]. Studies have shown that preoperative sarcopenia is linked to poor postoperative outcomes, including higher complication rates, longer hospital stays, and increased mortality across various oncological specialties^[4,5].

While various imaging modalities are available for sarcopenia assessment, preoperative CTA is widely used in abdominal flap breast reconstruction^[6]. A common approach is to measure the cross-sectional area of all relevant muscles at the L3 level, including the bilateral rectus abdominis, obliques, psoas, and paraspinal muscles^[4]. This method enables easy diagnosis, as the CTA protocol routinely includes the L3 level. Although there are other metrics, such as the frailty index, preoperative CTA also provides information that helps anticipate and manage potential complications.

In our previous study, Kim *et al.* assessed sarcopenia preoperatively using a validated method by calculating the skeletal muscle index (SMI) [Figure 1]; patients with an SMI below 38.5 were classified as sarcopenic^[7]. In a retrospective cohort of 463 patients undergoing abdominal-based flap breast reconstruction, multivariable analyses revealed that sarcopenia was independently associated with an increased incidence of complications, including breast hematoma, wound issues, abdominal functional weakness, and the need for reoperation^[7]. Identifying this increased risk of complications enables early patient counseling and meticulous preparation for surgical procedures to help mitigate these risks.

Bulge/hernia risk assessment (protrusion)

Postoperative bulges or hernias have been reported in 3% to 10% of patients who undergo abdomen-based microsurgical breast reconstruction^[8]. Several clinical factors, such as obesity, smoking, preoperative chemotherapy, muscle or fascia harvesting during operation, nerve sacrifice, and bilateral procedures, have been identified as potential risk factors for developing these complications^[9]. To reduce the risk, reinforcing the abdominal wall with synthetic or biological mesh is commonly recommended. When bulges or hernias occur, they not only significantly impact the patient's quality of life but also often require additional surgical intervention. Therefore, it is crucial to identify patients at higher risk in advance and take appropriate preventive measures.



Figure 1. Preoperative sarcopenia was evaluated by measuring the cross-sectional area of skeletal muscle at the L3 level. Patients with a SMI below 38.5 were classified as having sarcopenia, which is recorded in the volumetry sheet. SMI measured manually, without software assistance. SMI: Skeletal muscle index.

Efforts to identify risk factors detectable via CT have been ongoing. Tokumoto *et al.* found that a rectus abdominis thickness of less than 8 mm at the level of the umbilicus was associated with an increased risk of abdominal bulging^[9]. In a study by Kappos *et al.*, morphometric measurements from preoperative CTA - including a decreased cross-sectional area of rectus abdominis muscle at the L4 level and an increased inter-rectus abdominis distance (the distance between the medial edges of the left and right rectus muscles) - were identified as significant risk factors associated with postoperative bulging or hernia^[10]. Similarly, our study used CTA morphometric measures to assess the risk of bulging or hernia^[11]. It found that abdominal wall protrusion, measured as the maximum vertical distance from a line connecting both anterior superior iliac spines to the inner border of the abdominal wall in preoperative CTA images, was associated with an increased risk of bulging or hernia [Figure 2]. Additionally, their multivariable analysis revealed that older age and the use of lateral perforators were also associated with an increased risk. Using these factors, we developed a risk stratification scoring system called the Samsung Medical Center Risk Score for bulge/hernia. Patients aged 52 or older were assigned 3 points, those with lateral row perforators were given 4 points, and patients with an abdominal wall protrusion of 22.3 mm or greater received additional points based on the Charlson scoring system [Figure 2]^[11].

Using this classification system, surgeons at our institution are encouraged to take extra precautions when operating on patients at high risk of abdominal bulge or hernia. This includes prudent perforator selection and careful planning with precise, less-invasive pedicle harvest during abdominal flap elevation, focusing on

Category	Risk Score	
Age ≥ 52	0 or 3	Low-risk 0 Int.-risk 3,4 High-risk ≥ 7
Protrusion $\geq 22.3\text{mm}$	0 or 4	
Lateral row perforator	0 or 4	
Total score	0 - 11	

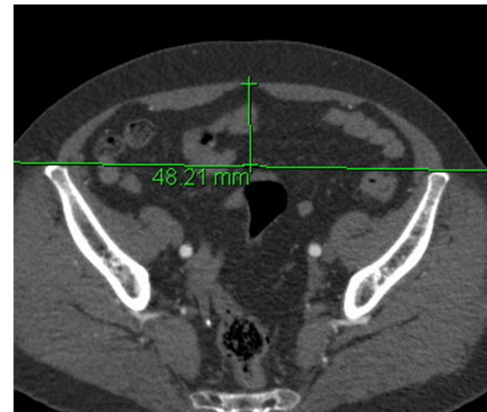


Figure 2. (Left) The table presents the Samsung Medical Center Risk Score for bulge/hernia, which is incorporated into the volumetry sheet. (Right) Abdominal wall protrusion is measured as the maximum vertical distance from a line connecting both anterior superior iliac spines to the inner border of the abdominal wall on preoperative CTA images. CTA: Computed tomography angiography.

preserving as much nerve, muscle, and fascia as possible. Additionally, meticulous fascia repair should be prioritized, with active consideration given to the use of mesh or acellular dermal matrix for reinforcement.

Step-off deformity risk assessment

The term “step-off deformity”, also referred to as residual abdominal overhang or localized fat excess, describes a suboptimal aesthetic outcome that can occur after autologous abdominal flap reconstruction^[12]. This condition is characterized by an irregular contour along the scar line where the upper and lower abdominal tissues meet, resulting in uneven and irregular contours^[13]. While it is a well-known issue in abdominoplasty^[14], data on its general incidence is limited, with only one study conducted at our institution to assess its incidence and associated risk factors.

In the study by the author, step-off deformity was observed in 20.3% of patients^[15]. The deformity was defined by the angle between the upper and lower abdominal tissues relative to the scar line in lateral view photographs, with an angle of less than 165° . Risk factors identified for the development of this deformity included a higher body mass index (BMI), the presence of a preoperative abdominal fold, and differences in thickness between the upper and lower abdominal flaps. The study suggested a BMI cut-off value of 26.1 and a thickness difference of 9.5 mm, as measured on preoperative axial CT images^[15].

Based on our research findings, we assess the thickness difference between the upper and lower abdominal flaps preoperatively using CTA images taken in an optimal position for surgical flap design [Figure 3]. By incorporating this risk assessment into preoperative counseling, we inform patients of potential risks. When the thickness difference exceeds 9.5 mm, we implement preventive strategies, such as extensive beveling of the upper abdominal flap during harvesting. We also employ cephalic-direction beveling on the caudal side of the flap and limit undermining, strategically redistributing beveled fat tissue during closure to address thickness variations and reduce the likelihood of step-off deformity.

FLAP PLANNING

Volumetry (donor/breast)

Measuring breast volume and the expected abdomen flap volume and determining the inset ratio are the most important initial steps in flap design. Depending on the inset ratio, decisions can be made regarding which perforator to use, how many perforators are needed, and the positions of the upper and lower

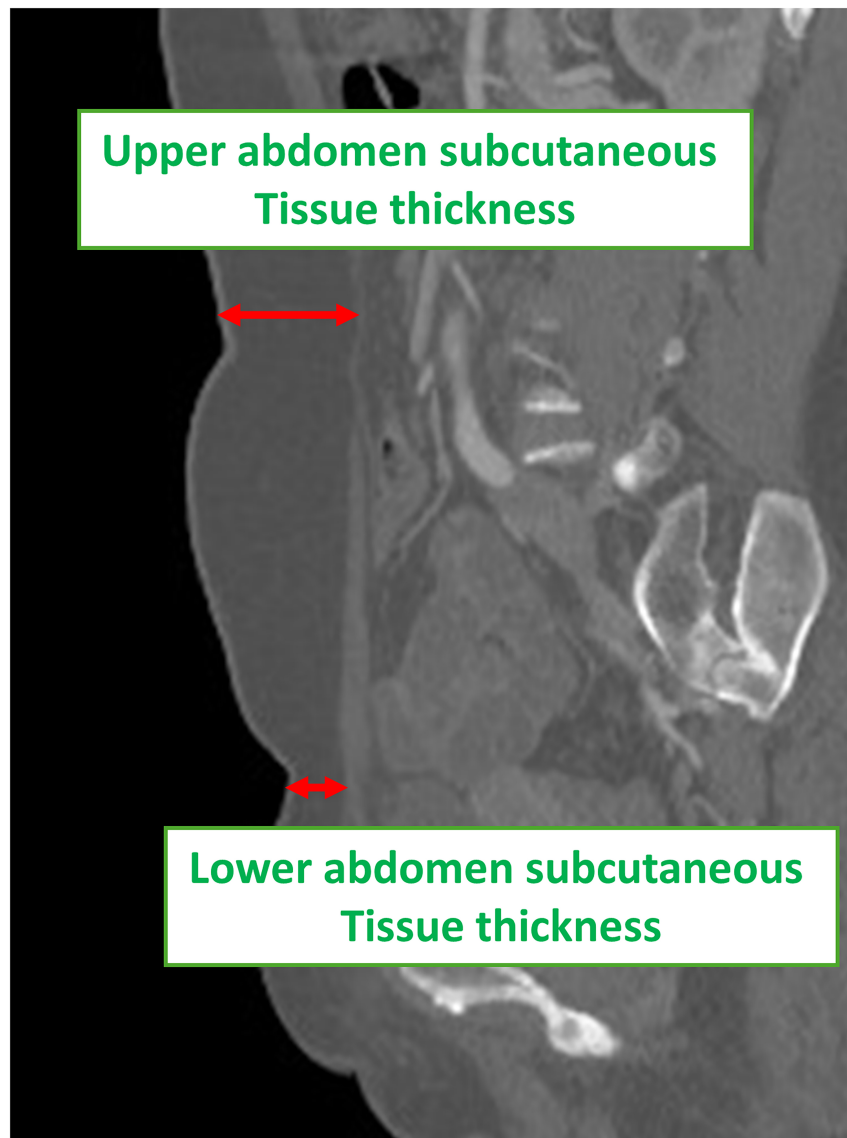


Figure 3. Preoperative CTA measured the maximum subcutaneous tissue thickness in the upper and lower abdominal regions, focusing on the umbilicus level and midway between the anterior superior iliac spine and pubic symphysis. Differences in thickness exceeding 9.5 mm were considered indicative of risk factors for developing a step-off deformity. CTA: Computed tomography angiography.

margins of the design. Insufficient volume can lead to asymmetry, while excessive volume may increase donor complications and the risk of flap fat necrosis and wound problems. Various imaging tools are utilized to measure abdominal fat volume and breast size. Although MRI is considered the most accurate, it is often not preferred due to its high cost, with other imaging methods being more cost-effective for routine assessments^[16].

At our clinic, we use a CT-based volumetric measurement method to optimize flap volume in breast reconstruction [Figure 4]. Axial CT images, covering the region from the clavicle to the abdomen, enable comprehensive volume assessments of both the breast tissue and desired abdominal fat tissue using a DICOM program. This enables the calculation of the breast-to-abdominal flap volume ratio^[17]. Based on this volumetric data, the authors adjust the vertical height of the abdominal flap design by a few centimeters to achieve the ideal tissue volume. Additionally, this approach provides flexibility in determining the flap size according to the ratio, allowing for more tailored adjustments. During inseting, these markings and the volumetric ratio enable more precise and efficient flap trimming. We found that applying the preoperative planning algorithm based on the inset ratio resulted in improved postoperative outcomes for patients^[18]. In addition to manually measuring the volume of each area, many programs now allow for volume measurements using DICOM files with 3D manipulation software, making the process more efficient [Figure 5].

Additionally, we use an application called deep inferior epigastric artery perforator (DIEP)-W, developed at our center, to predict abdominal flap volume^[19] [Figure 6]. This tool estimates the weight of the DIEP flap during breast reconstruction based on a formula derived from actual measured flap volumes. By measuring the thickness at 5 cm right, left and inferior from the umbilicus on a CT scan, the application simplifies and streamlines the process. Flap weight is calculated using six variables: the flap thickness at 3 points (mm), BMI of the patient (kg/m²), flap height (cm), and width (cm). Instead of manually measuring the area every centimeter on a CT scan - a time-consuming task - the application allows for a quick and easy estimation of the harvested flap's weight by inputting just this thickness measurement. Additionally, this calculation formula can be used to estimate how the flap volumes change according to the flap size.

Recipient vessel evaluation

Preoperative CTA enables a comprehensive assessment of recipient vessels by scanning from the clavicle level in a single continuous image. This imaging also allows for the detection of anatomical abnormalities in the recipient vessels. Importantly, preoperative CTA provides detailed information about the width and depth of each intercostal space, the diameter of the internal mammary artery (IMA)^[20], and the number of veins in each intercostal space. Although the internal mammary vein (IMV) is less well visualized than the artery, CTA can still aid in identifying its approximate diameter, number, and bifurcation level. Recognizing the level at which the IMV bifurcates enables surgeons to plan anastomoses at a proximal intercostal space before bifurcation, where a single larger vein is more likely to be present^[20,21]. Since the left side generally has smaller vessel diameters^[22], CTA provides valuable insight into how well the perforator will match and the degree of diameter discrepancy expected^[21,23].

In abdominal flap reconstruction, while the IMA remains the most commonly used recipient vessel, preoperative CTA enables the evaluation of all branches from the subscapular artery, as well as the lateral thoracic artery and thoracoacromial vessels [Figure 7]. With the increasing adoption of nipple-sparing mastectomy, the use of the thoracodorsal vessel as a recipient is also on the rise. Furthermore, if the IMA and thoracodorsal vessels are unsuitable or damaged, thoracoacromial or lateral thoracic vessels can be considered as alternative recipient vessels^[24] [Figure 8]. At our institution, although intra-flap anastomosis is typically performed for bipedicle flaps, preoperative CTA provides valuable information about secondary recipient vessel options when extra-flap anastomosis is necessary. It also assesses the course of the thoracoacromial vein, which can serve as a recipient vein for venous flow augmentation or superdrainage. By obtaining detailed information about various potential recipient vessels, we can not only plan which vessel to use, but also anticipate a backup plan in case any issues arise with the primary vessel during the procedure. This proactive approach helps ensure a smoother surgical process.

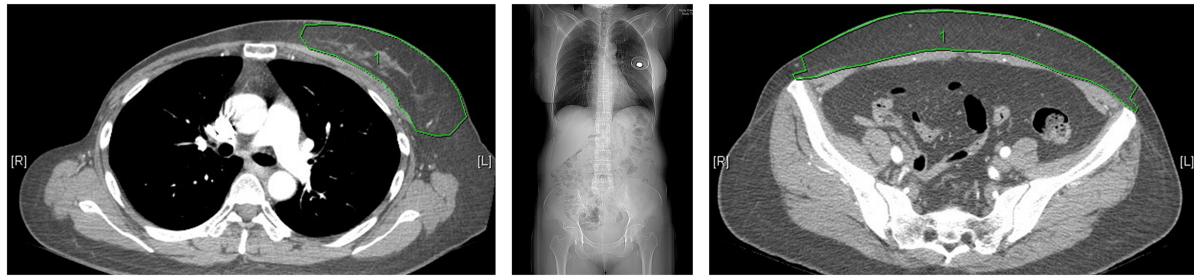


Figure 4. Measurement of breast volume (left) and DIEP flap volume (right) using computed tomographic angiography. The central image shows the scanned region, spanning from the clavicle to the abdomen, enabling comprehensive volume assessment. DIEP: Deep inferior epigastric artery perforator.

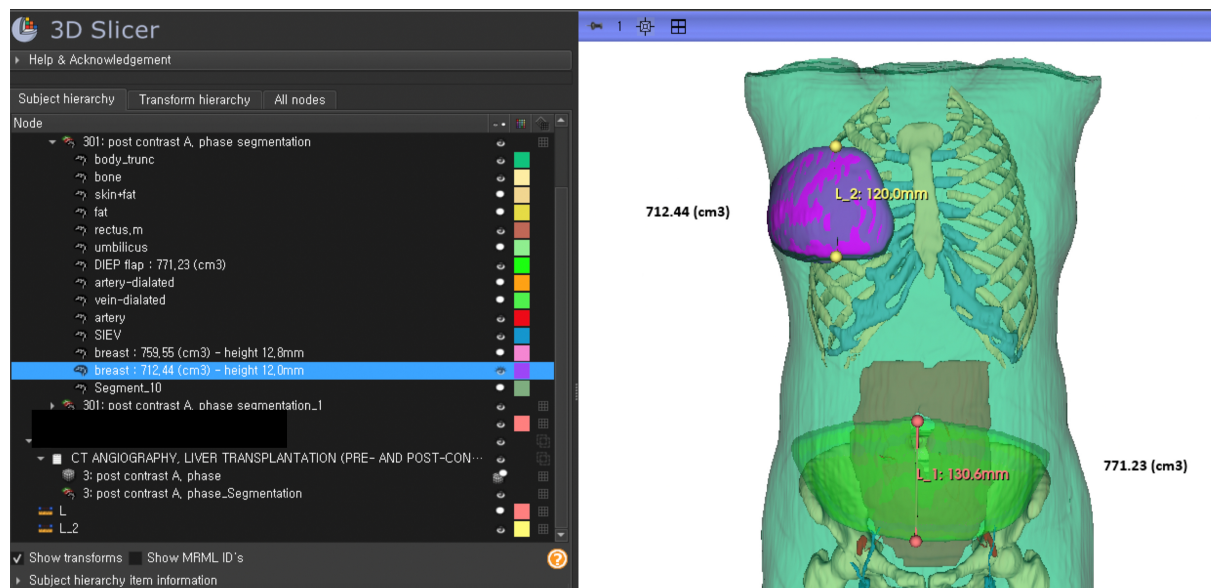


Figure 5. An example of volume measurement using DICOM files and 3D manipulation software.

Superficial vein evaluation

Venous drainage plays a significant role in the vascular complications faced by reconstructive breast surgeons^[25]. Unlike the arterial system, where the deep arteries dominate, the abdominal venous system is characterized by a dominant superficial drainage system^[26,27]. The superficial inferior epigastric vein (SIEV) is often evaluated when additional venous drainage is needed or to enhance venous outflow in a DIEP flap, and in rare cases, the superficial circumflex iliac vein (SCIV) may also be considered^[28]. Surgeons often choose the SIEV as the donor vein because it provides drainage from both the deep and superficial venous systems, with some reports indicating successful venous drainage using only the SIEV in DIEP flaps^[25]. Despite a patent deep inferior epigastric venous anastomosis, flap congestion has been reported in 2%~10% of cases, and SIEV superdrainage has been shown to reduce the risk of flap congestion and perfusion-related complications^[25,29,30].

Many surgeons routinely dissect and preserve SIEV during flap harvest to prevent complications, and use it as a lifeboat for additional venous drainage^[31], so understanding the vein's course can help reduce operative time. Coronal volume-rendered CTA images allow for easy identification of the SIEV's branching patterns and course on both sides [Figure 9], enabling precise mapping of the vein's location. This reduces the need

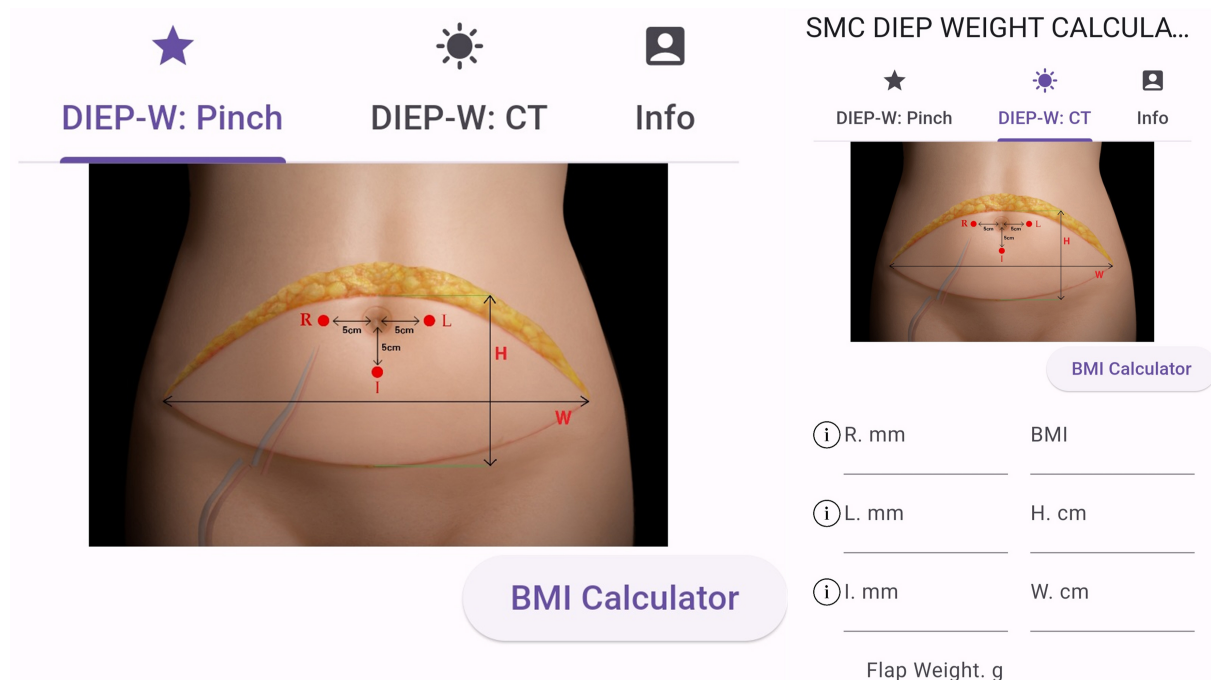


Figure 6. This figure shows the application interface of DIEP-W. CT: Computed tomography; BMI: body mass index.

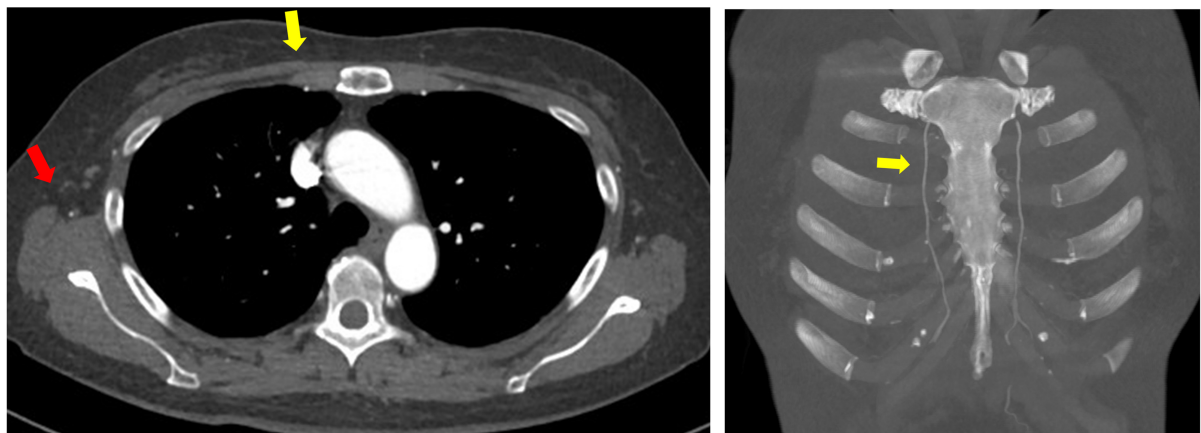


Figure 7. Three-dimensional reconstructed images showing vascular anatomy: (yellow arrow) the course and location of the internal mammary artery, and (red arrow) the preoperative tracing of the thoracodorsal vessels.

for extra caution in locating the SIEV during the inferior incision in DIEP flap harvesting, allowing surgeons to proceed with greater confidence and efficiency.

Selecting perforators with well-sized venous connections to the SIEV can reduce venous congestion and the need for superdrainage, thereby lowering the requirement for venous augmentation. At our institution, all CTA images are postprocessed into maximum intensity projection and three-dimensional volume-rendered images using the Aquarius Workstation (TeraRecon, Inc., San Mateo, Calif.)^[32]. Coronal volume-rendered images allow us to identify the branching patterns of bilateral SIEVs, such as single or bifurcating/more complex branches.

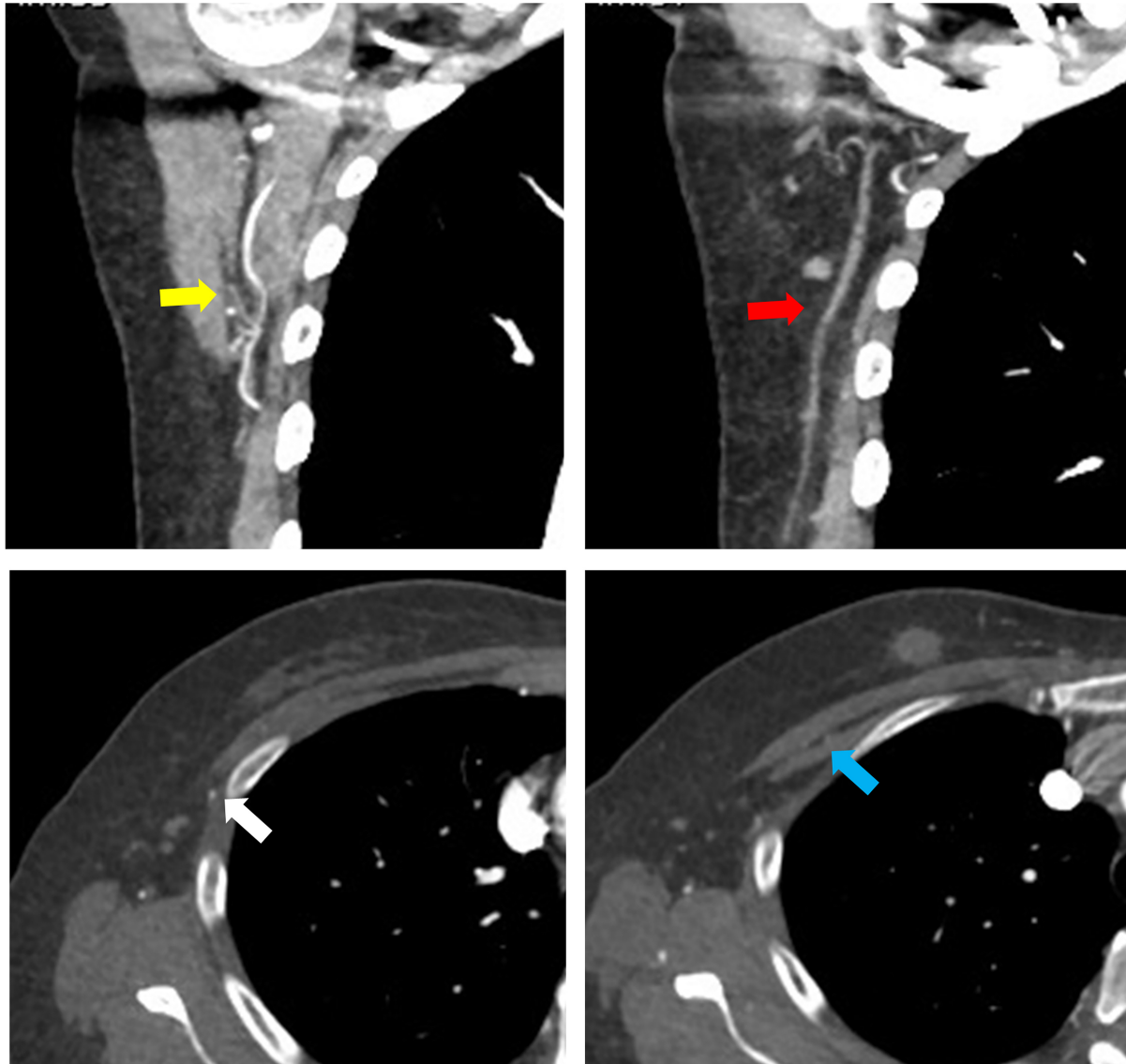


Figure 8. The yellow arrow indicates the subscapular vascular tree, the red arrow points to the lateral thoracic artery, the white arrow highlights the lateral thoracic vein, and the blue arrow shows the thoracoacromial vessels, all of which can be evaluated preoperatively using CTA. CTA: Computed tomography angiography.

When a dominant perforator is identified but lacks a direct connection or has only an indirect connection in preoperative CT planning, we evaluate the contralateral perforator's connecting vessel anatomy. In such cases, considering a change in pedicle laterality may be beneficial for unilateral breast reconstruction. If CTA reveals that a large SIEV lacks a direct connection to the deep inferior epigastric vein (DIEV) but shows a well-sized SIEA, opting for an SIEA flap instead of a DIEP flap can be a viable alternative to prevent venous congestion. When a preoperative Pfannestiel scar is present, superficial veins are often damaged, making it challenging to preserve the SIEV for superdrainage. However, our study reported that, as a compensatory response, direct communications between the SIEV and the DIEP venae comitantes increase, as does the overall number of connections, facilitating improved venous drainage^[32].

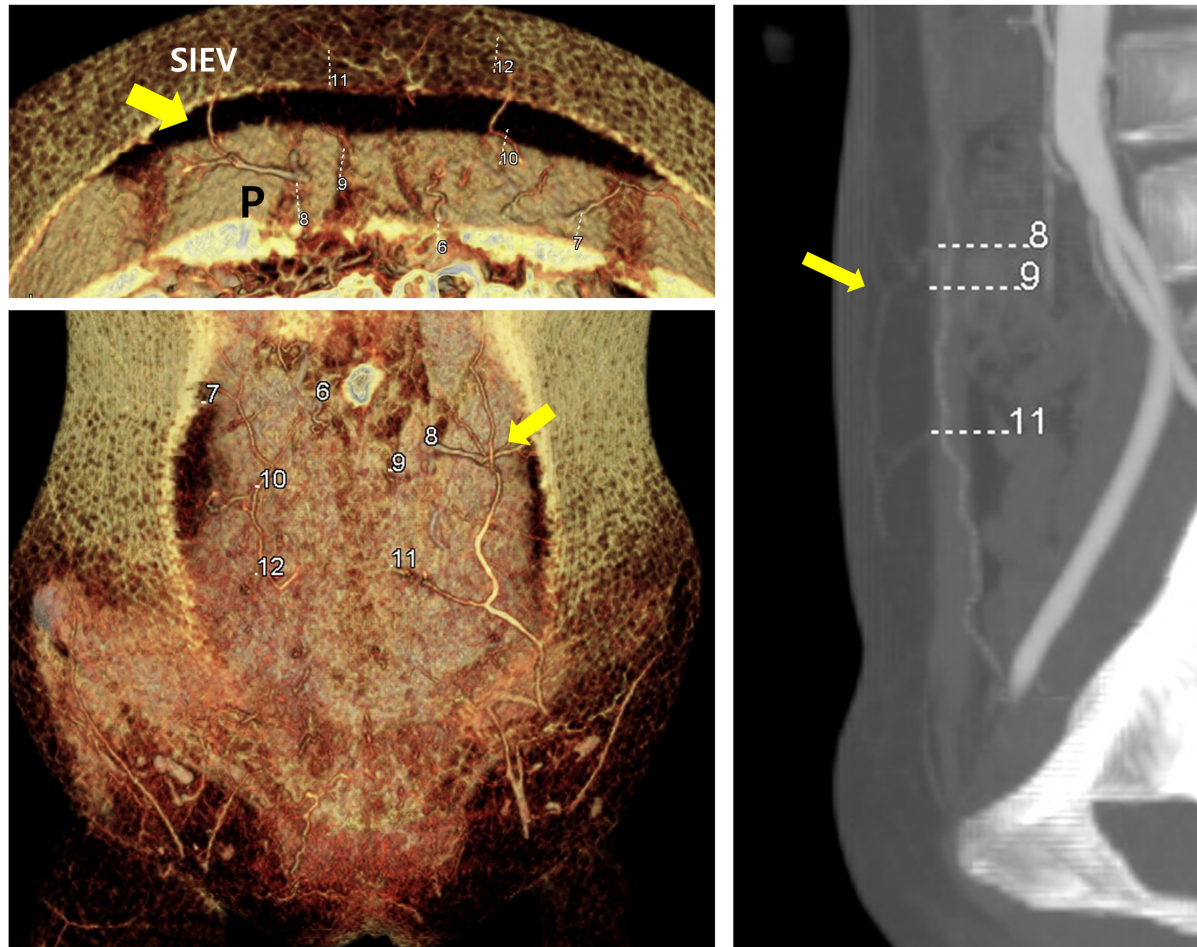


Figure 9. Volume-rendered images showing the communication between the SIEV and the deep inferior artery perforator. P, deep inferior epigastric artery perforator. The yellow arrow indicates the communication. SIEV: Superficial inferior epigastric vein.

SIEA flap/conjoined inguinal LN flap planning

The use of the superficial inferior epigastric artery (SIEA) flap helps reduce donor site complications, provides adequate flap volume, faster flap harvest time, and alleviates postoperative pain^[33]. However, due to significant anatomical variability observed in previous studies, such as the short vascular pedicle and small caliber of the SIEA, it is generally considered a secondary option for abdominal flap reconstruction.

Typically, a SIEA with a diameter greater than 1.5 mm is considered sufficient for use and does not cause a vessel diameter mismatch^[33,34]. However, preoperative assessment of superficial vessel diameter, including both the SIEA and the SIEV, is crucial for planning SIEA flap procedures. In an anatomical study using CTA by Rozen *et al.*, the SIEA was identified in 469 of 500 hemiabdomen (94% incidence), but only 120 of the 500 hemiabdomens had an SIEA diameter exceeding 1.5 mm^[35]. Preoperative CTA allows surgeons to assess the location, branching pattern, and diameter of these vessels, and a thorough understanding of both the deep and superficial arterial systems can guide optimal perforator selection^[34,36]. Henry *et al.* proposed an algorithm for planning SIEA flap breast reconstruction that combines preoperative CTA with intraoperative angiosome assessment^[33].

At our institution, when the SIEA diameter exceeds 1.5 mm on CTA, we plan and use the SIEA flap to enable faster flap harvest and reduce donor site complications. In most cases, when the CTA indicates that the SIEA is suitable, flap elevation has been performed without significant issues. By preoperatively identifying the precise course of the SIEA and SIEV, we have been able to facilitate smoother flap harvests. However, even if an appropriately sized SIEA/V is identified preoperatively via CTA and confirmed intraoperatively, the most important factor in deciding to proceed with SIEA flap elevation is the intraoperative assessment of the perfusion area using indocyanine green angiography, with temporary clamping of the DIEP [Figure 10]. The final decision is made only if the perfusion area is deemed sufficient. Additionally, unilateral use of the SIEA/V can expedite flap harvest and reduce overall surgery time in cases requiring a bipedicle flap, particularly when the expected inset ratio exceeds 0.75.

With the information obtained from SIEA/V, it is possible to assist with conjoined lymph node flap transfer. For patients with breast cancer-related lymphedema (BCRL), a combined approach using a DIEP flap and a vascularized inguinal lymph node free flap has proven effective in treating BCRL and improving quality of life^[37-39]. The inguinal lymph nodes are harvested from an area between the SCIV and SIEV, which corresponds to the region between the inguinal ligament and the groin crease. Intraoperative verification of volume-rendered CTA images can assist with surgical planning [Figure 11].

Zhang *et al.* demonstrated that multidetector-row CT angiography can accurately reveal the anatomical location and vascular supply of inguinal lymph nodes, including vessels like the SCIA/V and SIEA/V^[40]. This imaging enables precise mapping of lymph nodes, aiding in the selection of the optimal side for lymph node harvest. Building on this information, Demiri *et al.* proposed four types of chimeric DIEP and inguinal lymph node flaps based on CTA imaging, which support decisions on the mastectomy side, lymph node donor side, and the side with the dominant DIEA perforator^[41].

Bipedicle flap

The breast-to-flap volume ratio, which indicates the inset rate, can be calculated using the volumetric data from both the breast and flap obtained through preoperative CTA. This inset rate then guides specific operative planning. At our institution, if the expected inset rate exceeds 0.75, we plan a bipedicle flap utilizing two deep inferior epigastric artery pedicles from either side, without strict adherence to the rows and numbers of perforators, rather than opting for venous augmentation^[18,42]. The final decision to perform a bi-pedicle flap is made after intraoperative indocyanine green angiography, where the perfusion area is visualized by temporarily clamping the contralateral perforator. This algorithmic approach, as demonstrated in our study, has been shown to significantly reduce overall perfusion-related complications. In addition, conjoined bilateral flaps are actively considered for patients with a midline vertical scar on the lower abdomen from prior surgeries, particularly when the estimated inset ratio is greater than 0.5.

When planning a bipedicle DIEP flap, an approach that has gained popularity involves using an intraflap crossover anastomosis^[43]. This technique connects a branch of the primary flap's pedicle to the pedicle of the secondary pedicle, which is contralateral to the primary DIEA pedicle. This method improves the flap's maneuverability during inset by providing ample pedicle length. A key aspect of designing pedicle configurations for intraflap crossover is choosing the ideal primary DIEA pedicle and the suitable recipient site within it. The primary must offer reliable perforators for the primary flap's perfusion and have a sizable branch to serve as the recipient site for the intraflap crossover anastomosis with the contralateral pedicle. Careful anatomical consideration of the perforators, along with factors such as the topography of dominant perforators, the intramuscular DIEA branch pattern, side branch sizes, and the presence of superior DIEA continuations, is crucial for selecting the optimal primary pedicle. In this regard, preoperative CTA for

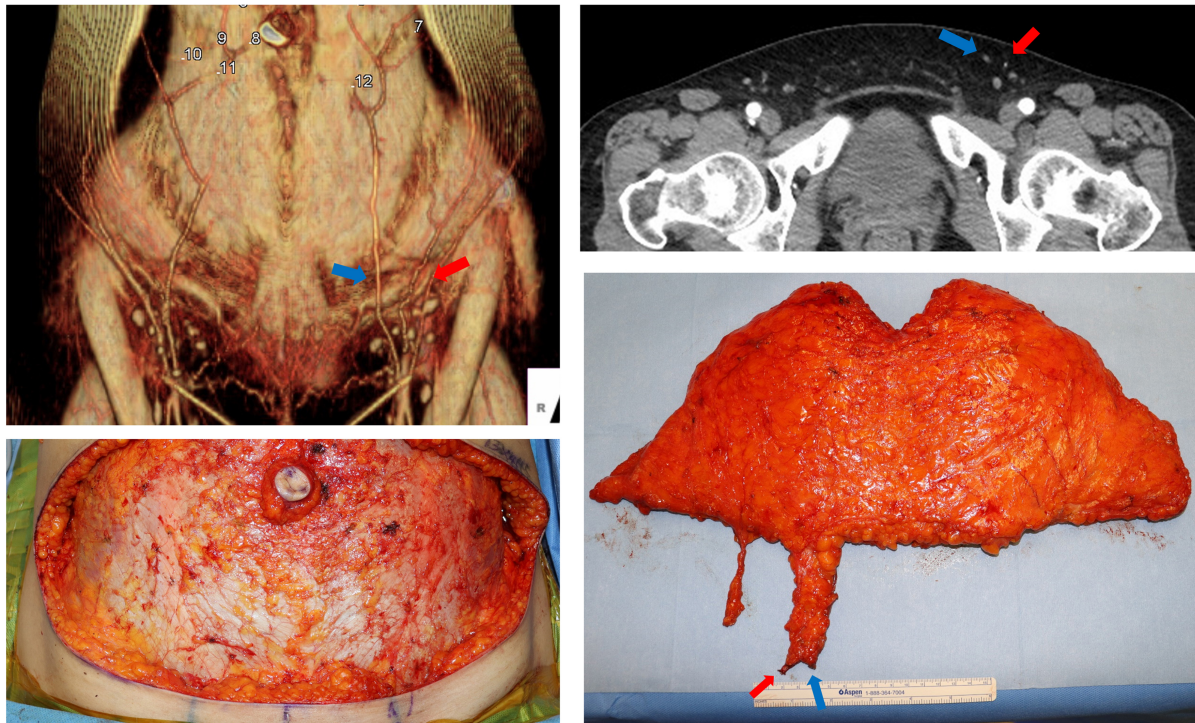


Figure 10. (Above) An SIEA flap was planned after identifying a suitable SIEA on preoperative CTA images. (Below) The course of the SIEA was traced on sagittal view images, and the flap was successfully harvested. Red arrow: SIEA; blue arrow: SIEV. CTA: Computed tomography angiography; SIEV: superficial inferior epigastric vein; SIEA: superficial inferior epigastric artery.

bipedicle planning offers precise information about the branching patterns of bilateral DIEAs, the locations of the dominant perforators, and the size of potential recipient vessels [Figure 12].

In our recent experience with 201 consecutive patients undergoing intraflap crossover anastomosis, the procedure proceeded as planned in 90% of cases based on preoperative CTA imaging^[17]. However, in the remaining cases, intraoperative adjustments were required, involving a switch of the primary pedicle. This was due to the fact that, despite CTA showing similar recipient vessel sizes on both sides, deviations from the initial plan became necessary during surgery. As these results suggest, thorough preoperative planning with CTA provides valuable information that can make the use of bipedicle DIEP flaps, which may initially seem challenging, more approachable and manageable.

Fasciotomy

Based on the information obtained from CTA, the surgeon selects the perforator that will provide the best perfusion for the flap. By tracing the selected perforator on the CT images, the surgeon can gather essential details for performing the fasciotomy. Preoperative CTA can provide anatomical data on the length of the intramuscular course of the harvested perforators, as well as the distance from the rectus muscle entry point of the most cranially located perforator to the branching point of the pedicle from the external iliac artery.

Based on the information gathered about fasciotomy length, if there are two or more perforators that seem capable of providing similar perfusion, the surgeon can choose the perforator with the expected shorter fasciotomy length to reduce the risk of donor site protrusion or hernia. At our institution, we use a short-fasciotomy technique to minimize the fasciotomy length, making only a minimal extension beyond the intramuscular course identified on CTA^[44] [Figure 13]. With this approach, the fasciotomy length closely

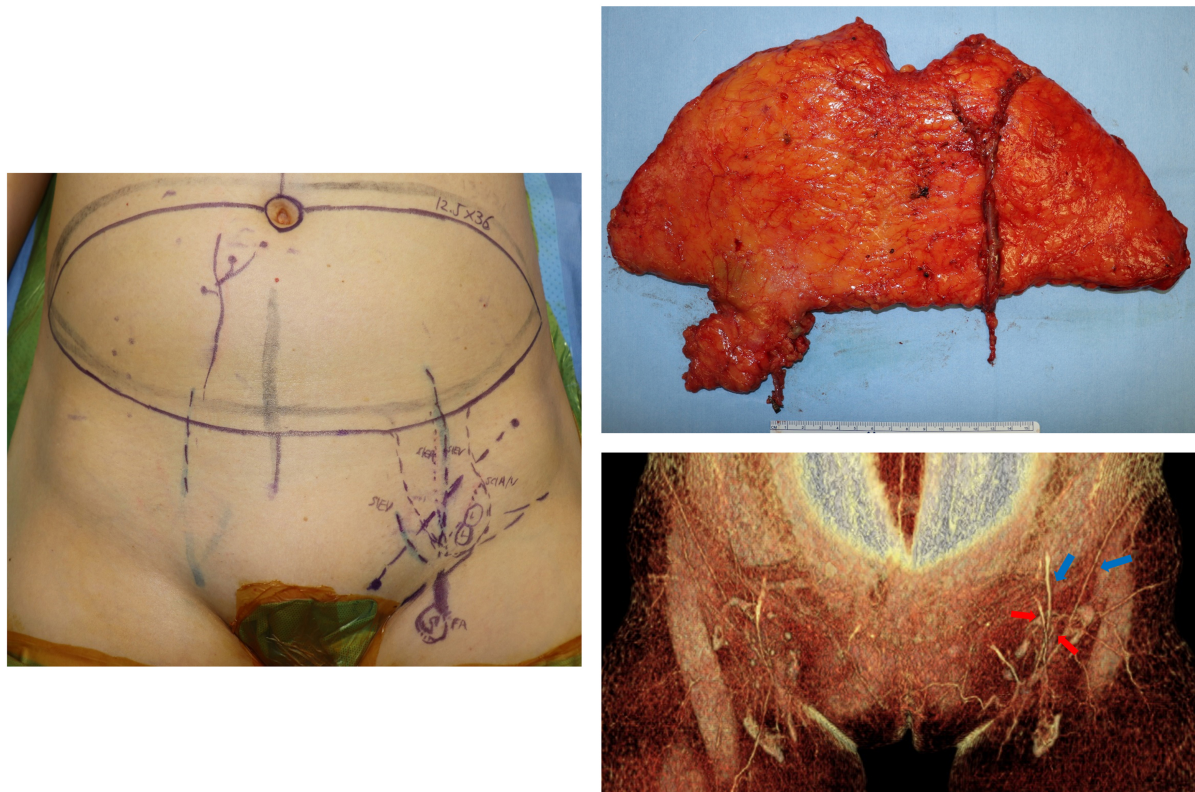


Figure 11. (Left) Design of the conjoint inguinal lymph node flap using the SIEA as the nutrient artery. (Right, above) Vascularized conjoint lymph node flap harvested according to preoperative planning. (Right, Below) Inguinal lymph nodes visible on preoperative CTA images, with the courses of the SCIA and SIEA identified. Red arrow: SIEA; blue arrow: SIEV. CTA: Computed tomography angiography; SIEV: superficial inferior epigastric vein; SIEA: superficial inferior epigastric artery.

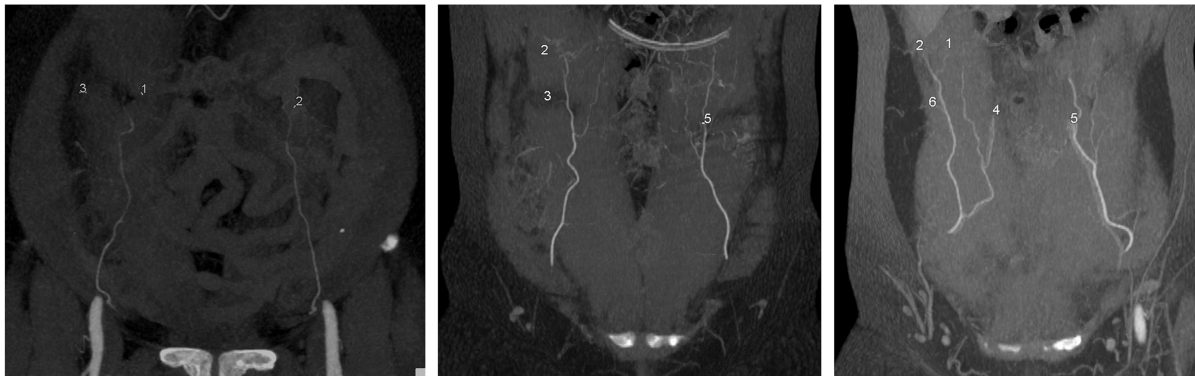


Figure 12. Three patterns of DIEA branching. (Left) Type I single branch. (Center) Type II bifurcating branch. (Right) Type III trifurcating branch. DIEA: Deep inferior epigastric artery.

matches the intramuscular length measured on CTA, enabling a smaller incision. This reduced incision size increases the likelihood of preserving nerves and muscles by reducing the risk of nerve dissection during the procedure.

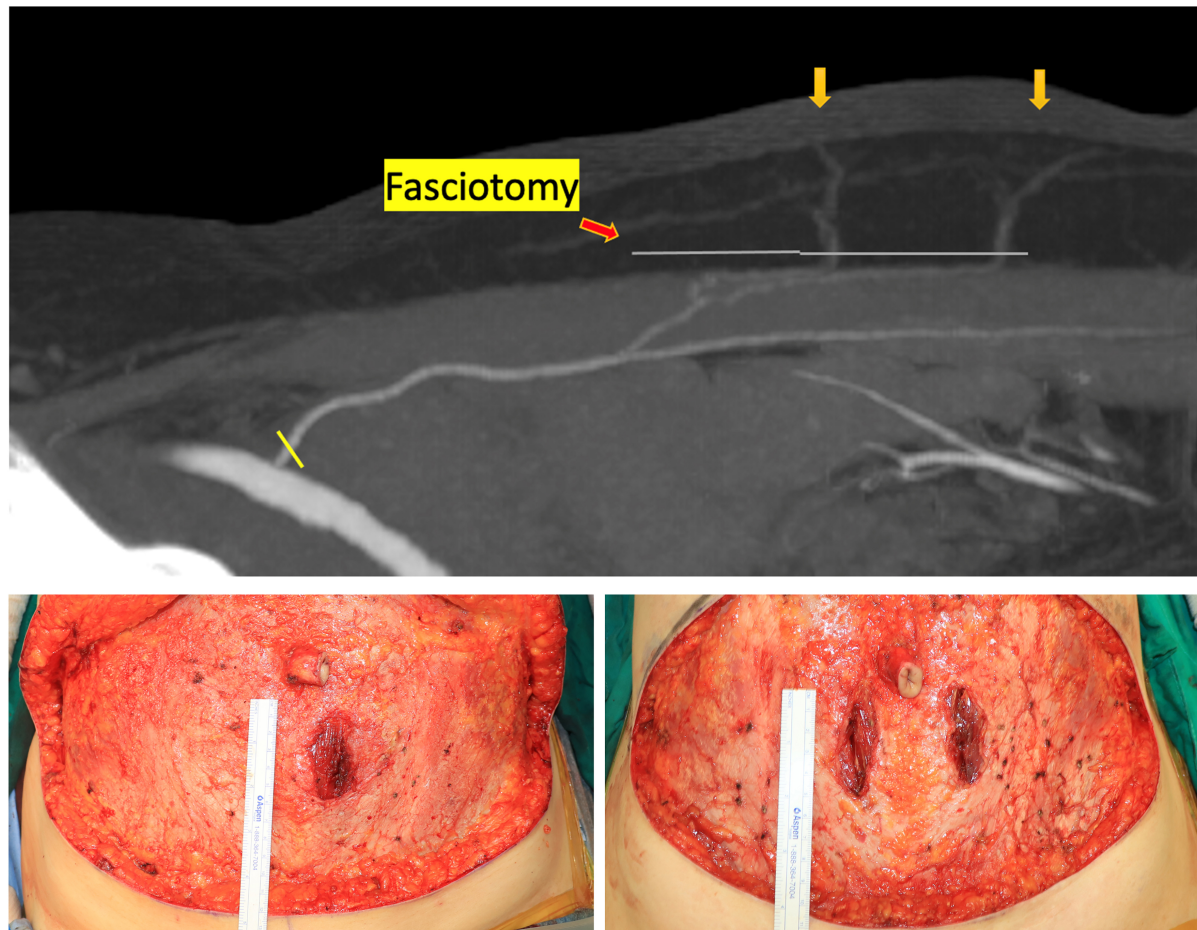


Figure 13. A fasciotomy is performed with only a minimal extension beyond the intramuscular course identified on CTA (above; the arrows indicate the length of the fasciotomy performed), followed by the result of the short-fasciotomy technique flap harvest (below). CTA: Computed tomography angiography.

CTA can also assist in selecting patients for DIEP flap harvest using a robotic approach^[45]. Robotic DIEP is being introduced as a surgical method to reduce donor morbidity by minimizing fascial incisions. In general, robotic DIEP is performed on patients with a short intramuscular course of the perforator. Kurlander *et al.* reported that CTA is a valuable tool for preoperative patient selection and for guiding robotic DIEP harvest, noting that 71% of hemi-abdomens in a study of 49 patients had suitable anatomy for robotic DIEP flap harvest^[46].

TRANSFERRING CT INFORMATION

When the information obtained from CTA imaging is accurately projected onto the actual patient, the time required for surgical planning can be dramatically reduced, allowing for more precise predictions of the perforator's location and course, which facilitates smoother dissections. Various methods have been attempted, with early attempts utilizing projectors to transfer CT image data. For example, Hummelink *et al.* used a handheld Pico projector (Philips, Eindhoven, the Netherlands) to project the information onto the patient^[47]. This projection technique has since been commercialized through an application that makes it more accessible and easier to use. At our institution, we employ a method that involves capturing a 3D reconstruction image from CTA and utilizing an augmented reality (AR) application for enhanced precision [Figure 14]. This tablet-based perforator-tracking AR visualization



Figure 14. Process of transferring the anatomy of interest onto the body surface using an AR application. AR: Augmented reality.

technique employs images that clearly show the reconstructed pathway of the perforator and the location of superficial veins. It projects this information onto the patient's body, using the ASIS and umbilicus as landmarks. This method has been reported to demonstrate very high accuracy, which aligns with the author's own experience in achieving precise and rapid perforator targeting.

In addition to the method used at our institution, other AR-based techniques have been proposed^[48,49], including using a synchronized 3D model that adjusts to the patient's real-time movement, transferring information via virtual reality (VR) technique, and visualizing the perforator's course through 3D printing. Seth *et al.* and Necker *et al.* introduced the use of AR headsets, such as the Microsoft HoloLens 2, to provide 3D visualization of the perforator course, enhancing surgical precision^[50,51]. VR systems such as VirSSPA and ImmersiveView VR have also been introduced for preoperative planning to enhance the visualization of perforator vessels. The method of using 3D printing to visualize anatomical pathways offers a more intuitive approach compared to AR or VR. By creating a 3D template, surgeons can physically handle and place it on the patient's body to verify the pathways directly in the operating room^[52]. This tactile feedback enhances visuospatial understanding, providing greater confidence during dissection. Studies have shown that 3D vascular mapping enables more accurate localization of perforators and branching patterns compared to using CTA alone, significantly reducing flap harvest time^[53,54]. In line with this, our institution has also adopted 3D printing to map not only the course of the DIEA but also the SIEV for surgical planning [Figure 15].

Beyond the accurate localization of perforators and vascular mapping, recent advances in 3D printing technology have enabled its use in shaping autologous tissue flaps with customized molds to improve

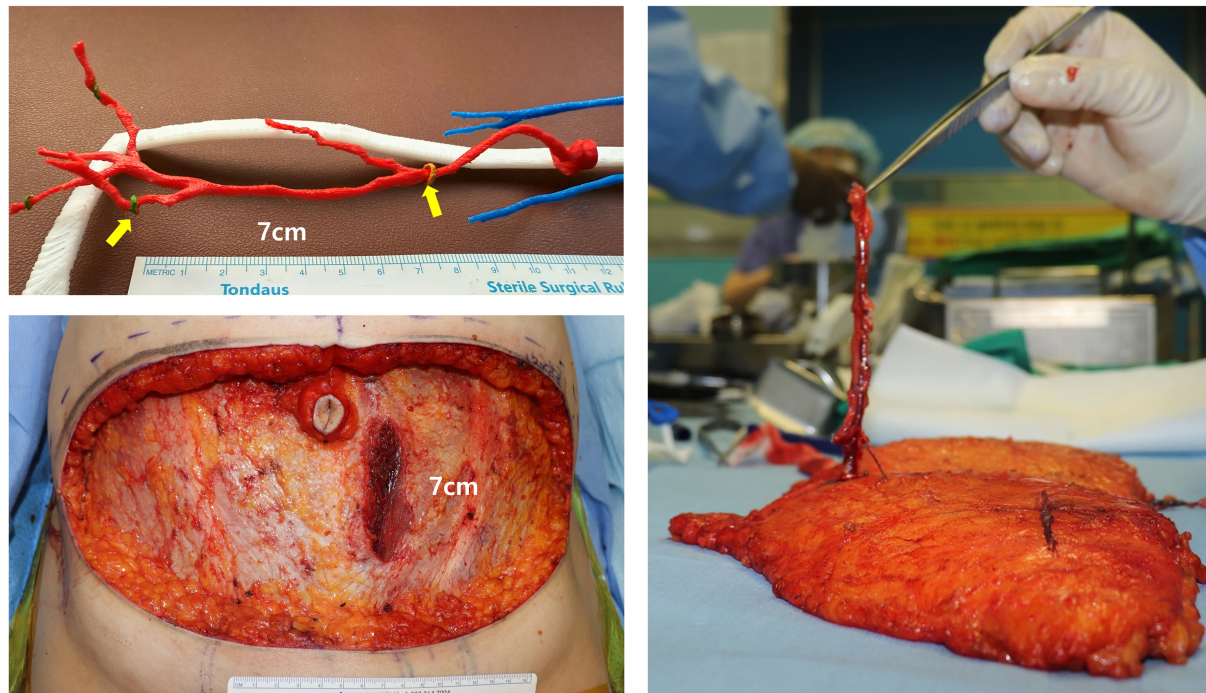


Figure 15. The pedicle, measured to have a 7 cm intramuscular course in 3D printing, was targeted for harvest using the short-fasciotomy technique. The fasciotomy length was precisely 7 cm, allowing for successful harvest.

aesthetic outcomes^[55]. Breast bio-models and breast molds generated from CTA or 3D scan-derived data have shown the potential in enhancing preoperative planning and intraoperative decision making^[56-59]. Studies have reported improved flap projection and symmetry in unilateral reconstructions using patient-specific models that mirror the contralateral breast^[56,58]. Furthermore, mold-based planning has been associated with high patient satisfaction, favorable cosmetic outcomes evaluated by surgeons, and accurate postoperative volume and width measurements^[57,59]. These findings support the integration of 3D printing into the preoperative workflow not only for anatomical visualization but also for surgical simulation and flap sculpting tailored to individual patient anatomy^[55].

CONCLUSION

Beyond simply selecting the optimal perforator and tracing the course of the DIEA in a preoperative setting, CTA imaging provides a wealth of information that can be applied clinically. In this paper, we explore the use of CTA in planning abdominal flap breast reconstruction, covering postoperative risk assessment, flap planning, and the transfer of this information into practice. By utilizing a single routine imaging modality preoperatively, we are able to obtain diverse information that enhances precision in planning. Detailed planning based on CTA data can facilitate the successful implementation of surgical plans and contribute to improved outcomes. Moreover, new technologies, such as AR and 3D printing, enable real-time application of CTA information in the operating room, further enhancing procedural accuracy. While protocols may vary between institutions, the valuable information provided by CTA remains indispensable, guiding surgeons through the challenges of abdominal flap harvesting and improving patient care in breast reconstruction.

DECLARATIONS

Authors' contributions

Substantial contributions to the conception and design of the review paper, including clinical recommendations, literature review, manuscript writing, and figure creation: Kim J, Woo KJ, Mun GH

Availability of data and materials

Not applicable.

Financial support and sponsorship

None.

Conflicts of interest

All authors declared that there are no conflicts of interest.

Ethical approval and consent to participate

Not applicable.

Consent for publication

Not applicable.

Copyright

© The Author(s) 2025.

REFERENCES

1. Teunis T, Heerma van Voss MR, Kon M, van Maurik JF. CT-angiography prior to DIEP flap breast reconstruction: a systematic review and meta-analysis. *Microsurgery*. 2013;33:496-502. DOI PubMed
2. Smit JM, Dimopoulou A, Liss AG, et al. Preoperative CT angiography reduces surgery time in perforator flap reconstruction. *J Plast Reconstr Aesthet Surg*. 2009;62:1112-7. DOI PubMed
3. Rosenberg IH. Sarcopenia: origins and clinical relevance. *J Nutr*. 1997;127:990S-1. DOI PubMed
4. Broyles JM, Smith JM, Phillips BT, et al. The effect of sarcopenia on perioperative complications in abdominally based free-flap breast reconstruction. *J Surg Oncol*. 2020;122:1240-6. DOI PubMed
5. Jain NS, Bingham E, Luvisa BK, et al. Sarcopenia best predicts complications in free flap breast reconstruction. *Plast Reconstr Surg Glob Open*. 2023;11:e5125. DOI PubMed PMC
6. Shafiee A, Bahri RA, Rafiei MA. Frailty among patients undergoing breast reconstruction surgery: a systematic review and meta-analysis. *J Plast Reconstr Aesthet Surg*. 2023;84:556-66. DOI PubMed
7. Kim S, Lee KT, Jeon BJ, Pyon JK, Mun GH. Association of preoperative sarcopenia with adverse outcomes of breast reconstruction using deep inferior epigastric artery perforator flap. *Ann Surg Oncol*. 2022;29:3800-8. DOI PubMed
8. Espinosa-de-Los-Monteros A, Frias-Frias R, Alvarez-Tostado-Rivera A, Caralampio-Castro A, Llanes S, Saldivar A. Postoperative abdominal bulge and hernia rates in patients undergoing abdominally based autologous breast reconstruction: systematic review and meta-analysis. *Ann Plast Surg*. 2021;86:476-84. DOI PubMed
9. Tokumoto H, Akita S, Kubota Y, Mitsukawa N. Relationship between preoperative abdominal wall strength and bulging at the abdominal free flap donor site for breast reconstruction. *Plast Reconstr Surg*. 2022;149:279e-86. DOI PubMed
10. Kappos EA, Jaskolka J, Butler K, O'Neill AC, Hofer SOP, Zhong T. Preoperative computed tomographic angiogram measurement of abdominal muscles is a valuable risk assessment for bulge formation after microsurgical abdominal free flap breast reconstruction. *Plast Reconstr Surg*. 2017;140:170-7. DOI PubMed
11. Park JW, Lee H, Jeon BJ, Pyon JK, Mun GH. Assessment of the risk of bulge/hernia formation after abdomen-based microsurgical breast reconstruction with the aid of preoperative computed tomographic angiography-derived morphometric measurements. *J Plast Reconstr Aesthet Surg*. 2020;73:1665-74. DOI PubMed
12. Walgenbach KJ, Shestak KC. "Marriage" abdominoplasty: body contouring with limited scars combining mini-abdominoplasty and liposuction. *Clin Plast Surg*. 2004;31:571-81. DOI PubMed
13. Stalder MW, Accardo K, Allen RJ, Sadeghi A. Aesthetic refinement of the abdominal donor site after autologous breast reconstruction. *Plast Reconstr Surg*. 2015;136:455-61. DOI PubMed
14. Stewart KJ, Stewart DA, Coghlan B, Harrison DH, Jones BM, Waterhouse N. Complications of 278 consecutive abdominoplasties. *J Plast Reconstr Aesthet Surg*. 2006;59:1152-5. DOI PubMed

15. Kim J, Son S, Mun GH. Risk factors for step-off deformity of the donor site following abdominal flap-based breast reconstruction. *Plast Reconstr Surg.* 2025;155:16e-25. DOI PubMed
16. Azzi AJ, Hilzenrat R, Viezel-Mathieu A, Hemmerling T, Gilardino M. A review of objective measurement of flap volume in reconstructive surgery. *Plast Reconstr Surg Glob Open.* 2018;6:e1752. DOI PubMed PMC
17. Kim JH, Lee KT, Mun GH. Optimizing intraflap anastomosis of conjoined bilateral DIEP flap for breast reconstruction: planning, execution, and outcomes in 201 patients. *Plast Reconstr Surg.* 2025;155:608-16. DOI PubMed
18. Lee KT, Mun GH. Volumetric planning using computed tomographic angiography improves clinical outcomes in DIEP flap breast reconstruction. *Plast Reconstr Surg.* 2016;137:771e-80. DOI PubMed
19. Woo KJ, Kim EJ, Lee KT, Mun GH. A novel method to estimate the weight of the DIEP flap in breast reconstruction: DIEP-W, a simple calculation formula using paraumbilical flap thickness. *J Reconstr Microsurg.* 2016;32:520-7. DOI PubMed
20. Cook JA, Tholpady SS, Momeni A, Chu MW. Predictors of internal mammary vessel diameter: a computed tomographic angiography-assisted anatomic analysis. *J Plast Reconstr Aesthet Surg.* 2016;69:1340-8. DOI PubMed
21. Kim H, Lim SY, Pyon JK, Bang SI, Oh KS, Mun GH. Preoperative computed tomographic angiography of both donor and recipient sites for microsurgical breast reconstruction. *Plast Reconstr Surg.* 2012;130:11e-20. DOI PubMed
22. Seth AK, Halvorson EG, Catterson SA, Carty MJ, Erdmann-Sager J. Left internal mammary vein size and its impact on microsurgical breast reconstruction. *Plast Reconstr Surg Glob Open.* 2022;10:e4704. DOI PubMed PMC
23. Kim H, Lim SY, Pyon JK, et al. Rib-sparing and internal mammary artery-preserving microsurgical breast reconstruction with the free DIEP flap. *Plast Reconstr Surg.* 2013;131:327e-34. DOI PubMed
24. Kim EJ, Lee HJ, Mun GH. Muscle-splitting approach to thoracoacromial vein for superdrainage in deep inferior epigastric artery perforator flap breast reconstruction. *Microsurgery.* 2019;39:228-33. DOI PubMed
25. Lee KT, Mun GH. Benefits of superdrainage using SIEV in DIEP flap breast reconstruction: a systematic review and meta-analysis. *Microsurgery.* 2017;37:75-83. DOI PubMed
26. Rozen WM, Pan WR, Le Roux CM, Taylor GI, Ashton MW. The venous anatomy of the anterior abdominal wall: an anatomical and clinical study. *Plast Reconstr Surg.* 2009;124:848-53. DOI PubMed
27. Bhullar H, Hughes K, Rozen WM, Rostek M, Hunter-Smith DJ. Demonstration of superficial venous dominance in the deep inferior epigastric perforator flap. *ANZ J Surg.* 2020;90:907-8. DOI PubMed
28. Lie KH, Taylor GI, Ashton MW. Hydrogen peroxide priming of the venous architecture: a new technique that reveals the underlying anatomical basis for venous complications of DIEP, TRAM, and other abdominal flaps. *Plast Reconstr Surg.* 2014;133:790e-804. DOI PubMed
29. Schaverien MV, Ludman CN, Neil-Dwyer J, et al. Relationship between venous congestion and intraflap venous anatomy in DIEP flaps using contrast-enhanced magnetic resonance angiography. *Plast Reconstr Surg.* 2010;126:385-92. DOI PubMed
30. Kim SY, Mun GH. Comments on “predicting venous congestion before DIEP breast reconstruction by identifying atypical venous connections on preoperative CTA imaging”. *Microsurgery.* 2019;39:571-2. DOI PubMed
31. Sadik KW, Pasko J, Cohen A, Cacioppo J. Predictive value of SIEV caliber and superficial venous dominance in free DIEP flaps. *J Reconstr Microsurg.* 2013;29:57-61. DOI PubMed
32. Kim SY, Lee KT, Mun GH. The influence of a Pfannenstiel scar on venous anatomy of the lower abdominal wall and implications for deep inferior epigastric artery perforator flap breast reconstruction. *Plast Reconstr Surg.* 2017;139:540-8. DOI PubMed
33. Henry FP, Butler DP, Wood SH, Jallali N. Predicting and planning for SIEA flap utilisation in breast reconstruction: an algorithm combining pre-operative computed tomography analysis and intra-operative angiosome assessment. *J Plast Reconstr Aesthet Surg.* 2017;70:795-800. DOI PubMed
34. Piorkowski JR, DeRosier LC, Nickerson P, Fix RJ. Preoperative computed tomography angiogram to predict patients with favorable anatomy for superficial inferior epigastric artery flap breast reconstruction. *Ann Plast Surg.* 2011;66:534-6. DOI PubMed
35. Rozen WM, Chubb D, Grinsell D, Ashton MW. The variability of the superficial inferior epigastric artery (SIEA) and its angiosome: a clinical anatomical study. *Microsurgery.* 2010;30:386-91. DOI PubMed
36. Zhang X, Mu D, Yang Y, et al. Predicting the feasibility of utilizing SIEA flap for breast reconstruction with preoperative BMI and computed tomography angiography (CTA) Data. *Aesthetic Plast Surg.* 2021;45:100-7. DOI PubMed
37. Chang EI, Masià J, Smith ML. Combining autologous breast reconstruction and vascularized lymph node transfer. *Semin Plast Surg.* 2018;32:36-41. DOI PubMed PMC
38. Forte AJ, Cinotto G, Boczar D, et al. Lymph node transfer combined with deep inferior epigastric perforators and transverse rectus abdominis myocutaneous procedures: a systematic review. *Gland Surg.* 2020;9:521-7. DOI PubMed PMC
39. Winters H, Tielemans HJP, Hummelink S, Slater NJ, Ulrich DJO. DIEP flap breast reconstruction combined with vascularized lymph node transfer for patients with breast cancer-related lymphedema. *Eur J Surg Oncol.* 2022;48:1718-22. DOI PubMed
40. Zhang H, Chen W, Mu L, et al. The distribution of lymph nodes and their nutrient vessels in the groin region: an anatomic study for design of the lymph node flap. *Microsurgery.* 2014;34:558-61. DOI PubMed
41. Demiri E, Dionysiou D, Kyriazidis I, Drougou A, Tsimponis A. Predesigned chimeric deep inferior epigastric perforator and inguinal lymph node flap for combined breast and lymphedema reconstruction: a comprehensive algorithmic approach. *JPRAS Open.* 2024;40:1-18. DOI PubMed PMC
42. Kim SY, Lee KT, Mun GH. Computed tomographic angiography-based planning of bipedicle DIEP flaps with intraflap crossover anastomosis: an anatomical and clinical study. *Plast Reconstr Surg.* 2016;138:409e-18. DOI PubMed

43. Koolen PG, Lee BT, Lin SJ, Erhard HA, Greenspun DT. Bipedicle-conjoined perforator flaps in breast reconstruction. *J Surg Res*. 2015;197:256-64. DOI PubMed
44. Kim J, Lee KT, Mun GH. Short fasciotomy-deep inferior epigastric perforator flap harvest for breast reconstruction. *Plast Reconstr Surg*. 2023;152:972e-84. DOI PubMed
45. Selber JC. The robotic DIEP flap. *Plast Reconstr Surg*. 2020;145:340-3. DOI PubMed
46. Kurlander DE, Le-Petross HT, Shuck JW, Butler CE, Selber JC. Robotic DIEP patient selection: analysis of CT angiography. *Plast Reconstr Surg Glob Open*. 2021;9:e3970. DOI PubMed PMC
47. Hummelink S, Hameeteman M, Hooegeveen Y, Slump CH, Ulrich DJ, Schultze Kool LJ. Preliminary results using a newly developed projection method to visualize vascular anatomy prior to DIEP flap breast reconstruction. *J Plast Reconstr Aesthet Surg*. 2015;68:390-4. DOI PubMed
48. Pereira N, Kufeke M, Parada L, et al. Augmented reality microsurgical planning with a smartphone (ARM-PS): a dissection route map in your pocket. *J Plast Reconstr Aesthet Surg*. 2019;72:759-62. DOI PubMed
49. Sullivan J, Skladman R, Varagur K, et al. From augmented to virtual reality in plastic surgery: blazing the trail to a new frontier. *J Reconstr Microsurg*. 2024;40:398-406. DOI PubMed
50. Seth I, Lindhardt J, Jakobsen A, et al. Improving visualization of intramuscular perforator course: augmented reality headsets for DIEP flap breast reconstruction. *Plast Reconstr Surg Glob Open*. 2023;11:e5282. DOI PubMed PMC
51. Necker FN, Cholok DJ, Shaheen MS, et al. The reconstructive metaverse - collaboration in real-time shared mixed reality environments for microsurgical reconstruction. *Surg Innov*. 2024;31:563-6. DOI PubMed PMC
52. Ghasroddashti A, Guyn C, Martou G, Edmunds RW. Utility of 3D-printed vascular modeling in microsurgical breast reconstruction: a systematic review. *J Plast Reconstr Aesthet Surg*. 2024;96:95-104. DOI PubMed
53. Jablonka EM, Wu RT, Mittermiller PA, Gifford K, Momeni A. 3-DIEPrinting: 3D-printed models to assist the intramuscular dissection in abdominally based microsurgical breast reconstruction. *Plast Reconstr Surg Glob Open*. 2019;7:e2222. DOI PubMed PMC
54. Mayer HF, Coloccini A, Viñas JF. Three-dimensional printing in breast reconstruction: current and promising applications. *J Clin Med*. 2024;13:3278. DOI PubMed PMC
55. Zhu KJ, Heron MJ, Zhu L, Seal SM, Mundy L, Broderick K. From printer to patient: a scoping review and new classification of ready-to-use three-dimensional printed constructs in autologous breast reconstruction. *J Plast Reconstr Aesthet Surg*. 2025;102:93-103. DOI PubMed
56. Chae MP, Hunter-Smith DJ, Spychal RT, Rozen WM. 3D volumetric analysis for planning breast reconstructive surgery. *Breast Cancer Res Treat*. 2014;146:457-60. DOI PubMed
57. Tomita K, Yano K, Hata Y, Nishibayashi A, Hosokawa K. DIEP flap breast reconstruction using 3-dimensional surface imaging and a printed mold. *Plast Reconstr Surg Glob Open*. 2015;3:e316. DOI PubMed PMC
58. Chae MP, Rozen WM, Patel NG, Hunter-Smith DJ, Ramakrishnan V. Enhancing breast projection in autologous reconstruction using the St Andrew's coning technique and 3D volumetric analysis. *Gland Surg*. 2017;6:706-14. DOI PubMed PMC
59. Hummelink S, Verhulst AC, Maal TJJ, Ulrich DJO. Applications and limitations of using patient-specific 3D printed molds in autologous breast reconstruction. *Eur J Plast Surg*. 2018;41:571-6. DOI PubMed PMC